Efficient Linear Solvers for Mortar Finite-Element Method

Tetsuji Matsuo[1], Yoshinori Ohtsuki[1,2], and Masaaki Shimasaki[1]

[1]Graduate School of Engineering, Kyoto University, Kyoto 615-8510, Japan
[2]Horiba, Ltd., Kyoto 601-8510, Japan

Efficient linear solvers for mortar finite-element method are studied. An analysis of a brushless DC motor shows that proposed preconditioners improve the convergence to the solutions of linear systems with and without Lagrange multipliers.

***Index Terms*—Lagrange multiplier, motor analysis, mortar finite-element method (FEM), preconditioner.**

I. Introduction

THE MORTAR finite-element method (FEM) [1], [2] is a domain decomposition approach that allows mesh nonconformity at the domain interfaces. It can provide an efficient formulation for analysis of rotating machinery using a sliding mesh [3]–[5].

The mortar FE formulation derives two types of linear systems of equations. One is a linear system with Lagrange multipliers [2]. The other is derived by eliminating the Lagrange multipliers [3]. A linear solver for an indefinite symmetric system is required to solve the former linear system because the Lagrange multiplier method results in a saddle-node problem. On the other hand, the latter system leads to a positive definite system of which coefficient matrix should not be obtained explicitly because of the computational cost. Several efficient linear solvers [6]–[8] have been proposed for these linear systems and applied to simple mortar FE analyses. However, efficient linear solvers for practical mortar FE analyses, such as motor analysis, have not been studied sufficiently. Comparison of linear solvers for the two types of linear systems with and without Lagrange multipliers is also required.

This study proposes several preconditioners to solve the two types of linear systems. The efficiencies of linear solvers using these preconditioners are compared.

II. Mortar FEM

A. Mortar FEM for Magnetostatic Field Analysis

A magnetostatic problem

$$\nabla \cdot (\nu \nabla A) = -J \tag{1}$$

is solved on a domain Ω. The domain Ω is divided into several subdomains each of which is triangulated. The triangulations do not necessarily match at interfaces between subdomains.

Digital Object Identifier 10.1109/TMAG.2007.891415

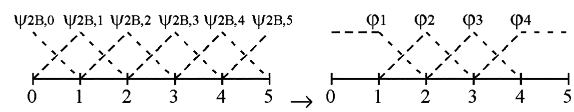

Fig. 1. Basis functions φ_k of mortar function space.

A weak form of (1) on a subdomain Ω_k is given as

$$\iint_{\Omega k} \nu \nabla A_k \cdot \nabla \psi_k \mathrm{d}\Omega = \iint_{\Omega k} J \psi_k \mathrm{d}\Omega \quad (\psi_k \in \Psi_k) \tag{2}$$

where Ψ_k is the space of piecewise linear FE functions corresponding to the triangulation of Ω_k.

For simplicity, it is assumed that the number of subdomains is 2 and that Ω_1 and Ω_2 are the mortar and nonmortar domains, respectively, for their interface Γ. The mortar FEM gives the boundary condition on Γ as a weak continuity condition (3)

$$\int_{\Gamma} (A_1 - A_2) \varphi \mathrm{d}\Gamma = 0 \quad (\varphi \in \vartheta). \tag{3}$$

In this equation, ϑ is the mortar function space of which basis functions are given by (4) (see Fig. 1)

$$\begin{aligned} \varphi_1 &= \psi_{2B,0} + \psi_{2B,1} \\ \varphi_N &= \psi_{2B,N} + \psi_{2B,N+1}, \\ \varphi_n &= \psi_{2B,n} \quad (n = 2, \ldots, N-1). \end{aligned} \tag{4}$$

Therein, $\psi_{2B,n}$ is the trace of $\psi_{2,n}$ on Γ corresponding to the node n, $\psi_{2,n}$ is a basis function of ψ_2, $N+1$ is the number of segments on the nonmortar side of Γ. From (3) and (4), the boundary condition is written as

$$\sum_{m=0}^{M+1} B_{1,i,m} A_{1B,m} - \sum_{n=0}^{N+1} B_{2,i,n} A_{2B,n} = 0 \quad (i = 1, \ldots, N) \tag{5}$$

where $M+1$ is the number of segments on the mortar side of Γ, $A_{kB,i}$ is the interface value of A_k on Ω_k, and

$$B_{k,i,j} = \int_{\Gamma} \psi_{k\mathrm{B},j} \varphi_i d\Gamma \quad (k = 1, 2). \tag{6}$$

B. Method of Lagrange Multipliers

Lagrange multipliers are often used to derive the linear system of equations for the mortar FE formulation (2) and (3). By defining the Lagrange multiplier space as

$$\lambda = \sum_{n=1}^{N} \lambda_n \varphi_n \tag{7}$$

the following formulation is obtained:

$$\iint_{\Omega 1} \nu \nabla A_1 \cdot \nabla \psi_1 d\Omega + \int_{\Gamma} \psi_1 \lambda d\Gamma = \iint_{\Omega 1} J \psi_1 d\Omega \tag{8}$$

$$\iint_{\Omega 2} \nu \nabla A_2 \cdot \nabla \psi_2 d\Omega - \int_{\Gamma} \psi_2 \lambda d\Gamma = \iint_{\Omega 2} J \psi_2 d\Omega \tag{9}$$

$$\int_{\Gamma} (A_1 - A_2) \varphi d\Gamma = 0 \tag{10}$$

where the number of subdomains is 2. These result in the following linear system of equations:

$$\begin{pmatrix} \boldsymbol{K}_1 & 0 & \boldsymbol{B}_1^{\mathrm{T}} \\ 0 & \boldsymbol{K}_2 & -\boldsymbol{B}_2^{\mathrm{T}} \\ \boldsymbol{B}_1 & -\boldsymbol{B}_2 & 0 \end{pmatrix} \begin{pmatrix} \boldsymbol{A}_1 \\ \boldsymbol{A}_2 \\ \boldsymbol{\lambda} \end{pmatrix} = \begin{pmatrix} \boldsymbol{F}_1 \\ \boldsymbol{F}_2 \\ 0 \end{pmatrix} \tag{11}$$

where

$$\boldsymbol{K}_k = \{K_{k,i,j}\} \quad \boldsymbol{B}_k = \{B_{k,i,j}\} \quad (k = 1, 2) \tag{12}$$

$$\boldsymbol{F}_k = \{F_{k,j}\} \quad \boldsymbol{A}_k = \{A_{k,j}\} \quad (k = 1, 2) \tag{13}$$

$$\boldsymbol{\lambda} = \{\lambda_j\}. \tag{14}$$

$$K_{k,i,j} = \iint_{\Omega k} \nu \nabla \psi_{k,} \cdot \nabla \psi_{k,j} \mathrm{d}\Omega \quad (k = 1, 2) \tag{15}$$

$$F_{k,j} = \iint_{\Omega k} J \psi_{k,j} \mathrm{d}\Omega \quad (k = 1, 2). \tag{16}$$

C. Method of Variable Elimination

The boundary condition (5) is rewritten as

$$\boldsymbol{A}_{2B} = \boldsymbol{C}\boldsymbol{A}_{1B} \tag{17}$$

where

$$\boldsymbol{C} = \boldsymbol{B}_{2B}^{-1} \boldsymbol{B}_{1B} \tag{18}$$

$$\boldsymbol{B}_{1B} = \begin{pmatrix} B_{1,1,0} & \cdots & B_{1,1,M+1} & -B_{2,1,0} & -B_{2,1,N+1} \\ \vdots & \ddots & \vdots & \vdots & \vdots \\ B_{1,N,0} & \cdots & B_{1,N,M+1} & -B_{2,N,0} & -B_{2,N,N+1} \end{pmatrix} \tag{19}$$

$$\boldsymbol{B}_{2B} = \begin{pmatrix} B_{2,1,1} & \cdots & B_{2,1,N} \\ \vdots & \ddots & \vdots \\ B_{2,N,1} & \cdots & B_{2,N,N} \end{pmatrix} \tag{20}$$

and A_{kB} is the interface values of $\boldsymbol{A}_k$ given by

$$\boldsymbol{A}_{1B} = (A_{1B,0}, \ldots, A_{1B,M+1}\ A_{2B,0}\ A_{2B,N+1})^{\mathrm{T}} \tag{21}$$

$$\boldsymbol{A}_{2B} = (A_{2B,1}, \ldots, A_{2B,N})^{\mathrm{T}}. \tag{22}$$

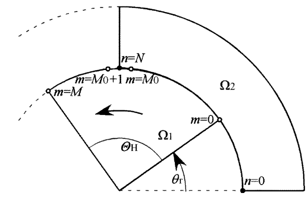

Fig. 2. Sliding interface between stator and rotator.

By using the relation (17), $\boldsymbol{A}_{2B}$ and λ are eliminated [3] from (8)–(10) as

$$\boldsymbol{Q}^{\mathrm{T}} \begin{pmatrix} \boldsymbol{K}_1 & 0 \\ 0 & \boldsymbol{K}_2 \end{pmatrix} \boldsymbol{Q} \begin{pmatrix} \boldsymbol{A}_{1\mathrm{I}} \\ \boldsymbol{A}_{1\mathrm{B}} \\ \boldsymbol{A}_{2\mathrm{I}} \end{pmatrix} = \boldsymbol{Q}^{\mathrm{T}} \begin{pmatrix} \boldsymbol{F}_1 \\ \boldsymbol{F}_2 \end{pmatrix} \tag{23}$$

where

$$\boldsymbol{Q} = \begin{pmatrix} 1 & 0 & 0 \\ 0 & 1 & 0 \\ 0 & \boldsymbol{C} & 0 \\ 0 & 0 & 1 \end{pmatrix} \tag{24}$$

and $\boldsymbol{A}_{kI}$ is the values of $\boldsymbol{A}_k$ other than $\boldsymbol{A}_{kB}$.

D. Weak Continuity between Stator and Rotator Domains

The mortar FEM is useful for analyses of rotating machines using sliding meshes.

Fig. 2 illustrates a sliding interface between rotator and stator, where m and n are the numbers of interface segments on rotator and stator sides, respectively; θ_r is the rotating angle and Θ_H is the half period along the azimuthal direction. A half-periodic boundary condition (25) is assumed

$$A(\theta + \Theta_H) = -A(\theta). \tag{25}$$

The present analysis assumes that the rotator side is the mortar side (Ω_1) and the stator side is the nonmortar one (Ω_2). The boundary condition of sliding interface is given by a weak continuity of (26), where the azimuthal coordinate is used [4], [5]

$$\int_0^{\Theta\mathrm{H}} \left\{ \sum_{m=0}^{M_0+1} A_{1m} \psi_{1\mathrm{B},m}(\theta - \theta_{\mathrm{r}}) - \sum_{m=M_0}^{M} A_{1m} \psi_{1\mathrm{B},m}\left(\theta - \theta_{\mathrm{r}} + \frac{\pi}{2}\right) - \sum_{n=0}^{N} A_{2n} \psi_{2\mathrm{B},n}(\theta) \right\} \varphi_i(\theta) \mathrm{d}\theta = 0 \quad (i = 1, \ldots, N). \tag{26}$$

Therein, the mortar nodes 0 to M_0 are in contact with the stator domain, and

$$A_{10} = -A_{1M} \quad A_{20} = -A_{2N} \tag{27}$$

$$\varphi_N = \psi_{2\mathrm{B},N} - \psi_{2\mathrm{B},0}$$
$$\varphi_n = \psi_{2\mathrm{B},n} \quad (n = 1, \ldots, N-1). \tag{28}$$

III. Linear Solvers

A. Method of Lagrange Multipliers

The coefficient matrix of (11) is indefinite. Accordingly, the MINRES (minimum residual) method is used to solve (11).

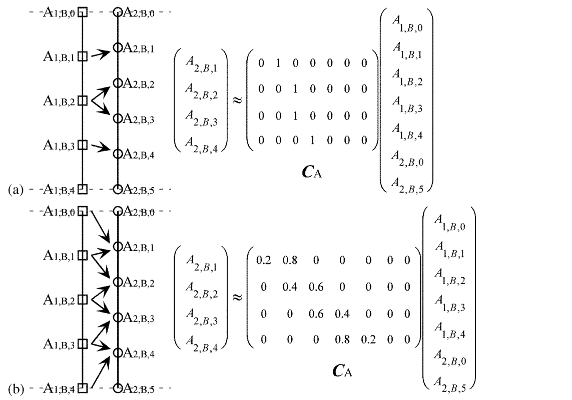

Fig. 3. Approximation of matrix $\boldsymbol{C}$ for preconditioning. (a) Point approximation. (b) Linear approximation.

The preconditioner in the form of Blockdiag ($\boldsymbol{M}_1$, $\boldsymbol{M}_2$, $\boldsymbol{M}_B$) is useful where $\boldsymbol{M}_1 \approx K_1$, $\boldsymbol{M}_2 \approx \boldsymbol{K}_2$ and $\boldsymbol{M}_B \approx \boldsymbol{B} = \boldsymbol{B}_1\boldsymbol{K}_1^{-1}\boldsymbol{B}_1^{\mathrm{T}} + \boldsymbol{B}_2\boldsymbol{K}_2^{-1}\boldsymbol{B}_2^{\mathrm{T}}$ [9]. This study approximates $\boldsymbol{B}$ as follows.

i) $\boldsymbol{K}_1$ and $\boldsymbol{K}_2$ are approximated by $\mathrm{diag}(\boldsymbol{K}_1)$ and $\mathrm{diag}(\boldsymbol{K}_2)$.
ii) $\boldsymbol{B}$ given by i) is approximated by $\mathrm{diag}(\boldsymbol{B})$.
iii) $\boldsymbol{K}_1$ and $\boldsymbol{K}_2$ are approximated by their IC decompositions.
iv) $\boldsymbol{B}$ given by iii) is approximated by $\mathrm{diag}(\boldsymbol{B})$.
v) $\boldsymbol{B}$ given by iii) is approximated by dropping its elements at positions where elements of $\boldsymbol{B}_1\boldsymbol{B}_1^{\mathrm{T}} + \boldsymbol{B}_2\boldsymbol{B}_2^{\mathrm{T}}$ are 0 [the nonzero pattern of approximated $\boldsymbol{B}$ becomes the same as that for i)].

$\boldsymbol{M}_1, \boldsymbol{M}_2$, and $\boldsymbol{M}_{\mathrm{B}}$ are given, respectively, by IC decompositions of $\boldsymbol{K}_1$, $\boldsymbol{K}_2$, and approximated $\boldsymbol{B}$.

B. Method of Variable Elimination

When the linear system (23) is large, the matrix $\boldsymbol{C}$ should not be computed explicitly because it is dense. This paper proposes preconditioners using approximations $\boldsymbol{C}_{\mathbf{A}} \approx \boldsymbol{C}$ to solve (23). The matrix $\boldsymbol{C}$ represents a relation from $\boldsymbol{A}_{1B}$ on mortar nodes to $\boldsymbol{A}_{2B}$ on nonmortar nodes. This study gives $\boldsymbol{C}_{\mathbf{A}}$ so as to approximate each element of $\boldsymbol{A}_{2B}$ as follows:

i) value of $\boldsymbol{A}_{1B}$ at the nearest node on the mortar side (point approximation);
ii) linearly interpolated from the values of $\boldsymbol{A}_{1B}$ at the two adjacent nodes on the mortar side (linear approximation).

Fig. 3 illustrates these approximations for preconditioning.

An approximated coefficient matrix of linear system (23) using $\boldsymbol{C}_{\mathbf{A}}$ is IC decomposed for preconditioning to solve (23) using the CG method.

IV. Numerical Examination

A. Simple Problem

First, a 2-D magnetostatic field in an iron core shown in Fig. 4(a) is analyzed. The analyzed domain is subdivided into two subdomains Ω_1 and Ω_2 as shown in Fig. 4(b). The interface between them is subdivided into 200 and 194 segments on the mortar and nonmortar sides, respectively. The subdomains Ω_1 and Ω_2 are subdivided into $200 \times 100 \times 2$ and $194 \times 97 \times 2$ triangular elements, respectively.

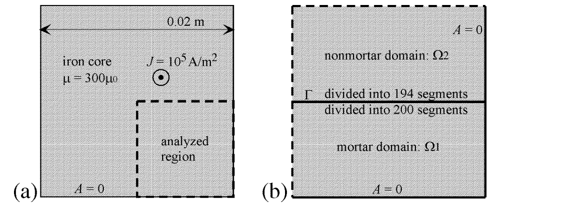

Fig. 4. Approximation of matrix $\boldsymbol{C}$: (a) analyzed iron core and (b) mortar and nonmortar domains.

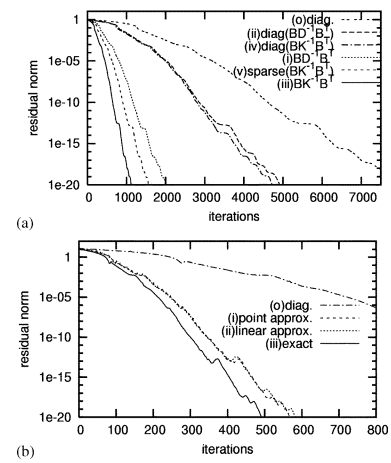

Fig. 5. Convergence to solution for analysis of iron core: (a) method of Lagrange multipliers and (b) method of variable elimination.

TABLE I
COMPARISON OF COMPUTATIONAL COST FOR ANALYSIS OF IRON CORE: (a) METHOD OF LAGRANGE MULTIPLIERS AND (b) METHOD OF VARIABLE ELIMINATION

(a)

	(o)	(i)	(ii)	(iii)	(iv)	(v)
# of iterations	7963	2006	4920	1120	4727	1565
comp. time(s)	308	147	360	92	353	120

(b)

	(o)	(i)	(ii)	(iii)	FEM
# of iterations	1716	585	570	493	482
comp. time(s)	69	41	40	47	33

Equations (11) and (23) are solved using the preconditioners proposed in the Section III. Fig. 5 shows the convergences to their solutions. Table I compares the iterations and computation times for the convergences. Columns "(o)" show a simple diagonal preconditioning; column (iii) of (b) is given by the preconditioner using exactly computed $\boldsymbol{C}$ for the method of variable elimination. For comparison, the convergence of the conventional Galerkin FEM with $200 \times 200 \times 2$ elements is shown by column "FEM," where the ICCG method is used for the solution. The convergence criterion is 10^{-20} for the residual norm. A PC with Intel Pentium II (450 MHz) processor was used for the computation.

Fig. 4(a) and Table I(a) show that the preconditioners (iii) and (iv) are effective for the linear system with Lagrange multipliers whereas the preconditioners (ii) and (iv) using diagonal M_B are not very effective. However, when the system becomes large, preconditioner (iii) will be expensive because $\boldsymbol{M}_B$ for (iii) is dense.

On the other hand, Table I(b) shows that the proposed preconditioners (i) and (ii) for the method of variable elimination efficiently obtain the solution without a large increase in iterations compared with (iii). The increases in computation time and iterations are not large compared with the conventional FEM.

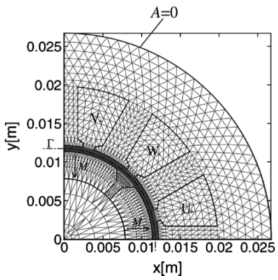

Fig. 6. Analyzed motor model.

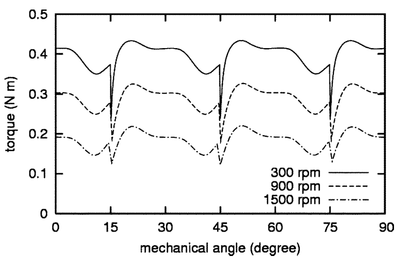

Fig. 7. Torque waveforms.

Fig. 4 and Table I also shows that the method of variable elimination can obtain the solution faster than the method of Lagrange multipliers.

B. A Motor Analysis

A magnetic field in a permanent-magnet brushless DC motor is analyzed with a sliding mesh. Fig. 6 illustrates the analyzed motor model (37.5-mm thick). The relative permeability of iron core is 1000. The magnetization of permanent magnet is 0.9 T. The half azimuthal period of 90° is equally divided into 90 segments at the interface between the stator and rotator. A PC with Intel Celeron (2 GHz) processor was used for the computation.

Fig. 7 shows torque waveforms obtained for rotating speed of 300, 900, and 1500 r/min, where smooth waveforms are obtained in spite of the mesh nonconformity. Fig. 8 shows the convergences to their solutions when $\theta_r = 22.5°$. Table II compares the iterations and computation times for the convergences. Table II(c) lists those in the case of $\theta_r = 0$ degree where mesh nonconformity does not occur at the interface. The conventional FEM using the ICCG method is also examined when $\theta_r = 0$ for comparison.

Fig. 8 and Table II show that the proposed preconditioner (v) is effective for the linear system with Lagrange multipliers, and that preconditioners (i) and (ii) proposed for the method of variable elimination efficiently obtain the solution. The method of variable elimination obtains the solution faster than the method of Lagrange multipliers. Table II(c) shows that the computational cost of the Mortar FEM is not much larger than that of the conventional FEM.

V. Conclusion

Efficient preconditioners are proposed for linear systems with and without Lagrange multipliers that result from the mortar FEM. An analysis of a brushless DC motor shows that proposed preconditioners improve the convergence to the solutions of both linear systems. The method of variable elimination can obtain the solution faster than the method of Lagrange multipliers.

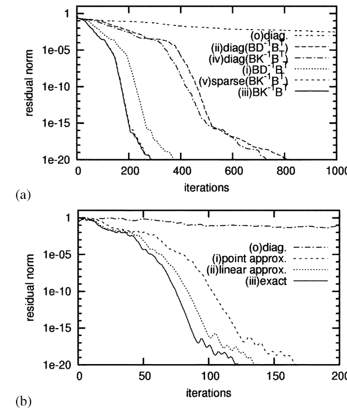

Fig. 8. Convergence to solution for motor analysis. (a) Method of Lagrange multipliers. (b) Method of variable elimination.

TABLE II
COMPARISON OF COMPUTATIONAL COST FOR MOTOR ANALYSIS: (a) LAGRANGE MULTIPLIER METHOD; (b) METHOD OF VARIABLE ELIMINATION; (c) METHOD OF VARIABLE ELIMINATION ($\theta_r = 0$)

(a)

	(o)	(i)	(ii)	(iii)	(iv)	(v)
# of iterations	$>10^4$	384	832	291	754	296
comp. time(s)	>3.5	0.28	0.59	0.28	0.56	0.25

(b)

	(o)	(i)	(ii)	(iii)
# of iterations	3102	168	136	124
comp. time(s)	1.2	0.13	0.11	0.24

(c)

	(o)	(i)	(ii)	(iii)	FEM
# of iterations	3047	123	121	121	123
comp. time(s)	1.1	0.09	0.09	0.22	0.08

Acknowledgment

This work was supported in part by the Japan Society for the Promotion of Science under Grant-in-Aid for Scientific Research (C), 17560255.

References

[1] C. Bernardi, Y. Maday, and A. T. Patera, "A new nonconforming approach to domain decomposition: The mortar element method," in *Nonlinear Partial Differential Equations and Their Applications*. White Plains, NY: Longman, 1994, pp. 13–51.

[2] F. B. Belgacem, "The mortar finite element method with Lagrange multipliers," *Numer. Math.*, vol. 84, pp. 173–197, 1999.

[3] F. Rapetti, F. Bouillault, L. Santandrea, A. Buffa, Y. Maday, and A. Razek, "Calculation of eddy currents with edge elements on non-matching grids in moving structures," *IEEE Trans. Magn.*, vol. 36, pp. 1351–1355, Jul. 2000.

[4] A. Buffa, Y. Maday, and F. Rapetti, "A sliding mesh-mortar method for a two dimensional eddy currents model for electric engines," *Mod. Math. Anal. Numer.*, vol. 35, no. 2, pp. 191–228, 2001.

[5] O. J. Antunes, J. P. A. Bastos, N. Sadowski, A. Razek, L. Santandrea, F. Bouillault, and F. Rapetti, "Using hierarchic interpolation with mortar element method for electrical machines analysis," *IEEE Trans. Magn.*, vol. 41, no. 5, pp. 1472–1475, May 2005.

[6] Y. Achdou, Y. Maday, and O. B. Widlund, "Iterative substructuring preconditioners for mortar element methods in two dimensions," *SIAM J. Numer. Anal.*, vol. 36, no. 2, pp. 551–580, 1999.

[7] J. Gopalakrishnan and J. E. Pasciak, "Multigrid for the mortar finite element method," *SIAM J. Numer. Anal.*, vol. 37, no. 3, pp. 1029–1052, 2000.

[8] M. Dryja, A. Gantner, O. B. Widlund, and B. I. Wohlmuth, "Multilevel additive Schwarz preconditioner for nonconforming mortar finite element methods," *J. Numer. Math.*, vol. 12, no. 1, pp. 23–38, 2004.

[9] H. C. Elman, "Preconditioners for saddle point problems arising in computational fluid dynamics," *Appl. Numer. Math.*, vol. 43, pp. 75–89, 2002.

Manuscript received April 24, 2006 (e-mail: tmatsuo@kuee.kyoto-u.ac.jp).